

Tropical tree species discrimination using very high-resolution satellite images and texture analysis

Matheus Pinheiro Ferreira¹
Yosio Edemir Shimabukuro¹
Carlos Roberto de Souza Filho²

¹Instituto Nacional de Pesquisas Espaciais - INPE
Caixa Postal 515 - 12245-970 - São José dos Campos - SP, Brasil
{mpf, yosio}@dsr.inpe.br

²Universidade Estadual de Campinas - UNICAMP
Caixa Postal 6152 - 13083-970 - Campinas - SP, Brasil
beto@ige.unicamp.br

Abstract. In this study, we evaluate the use of texture descriptors obtained from very high-resolution satellite imagery to improve tree species classification in a tropical forest. Gray level co-occurrence matrix (GLCM), gabor and wavelet features were combined with reflectance bands of the WorldView-2 (WV-2) and QuickBird-2 (QB-2) satellite sensors to perform species classification. The use of QB-2 and WV-2 reflectance data yielded 26.6% and 44.8% of average accuracy, respectively. Texture features combined with QB-2 bands did not improve significantly the results. However, the combination of GLCM features with WV-2 reflectance bands increased the average accuracy up to 5.7%, exceeding 15% for some species. Pioneer species such as *Cecropia hololeuca* and climax species such as *Cariniana legalis* were classified with approximately 90% accuracy. The results highlight the potential use of WV-2 imagery to monitor tropical forest environments.

Keywords: WorldView-2, QuickBird-2, Tropical forest.

1. Introduction

Tree species discrimination and mapping in tropical environments provides valuable insights for forest managers and nature conservationists. For example, forest restoration programs can take advantage of species maps to optimize the collection of seeds for seedling production. Moreover, indicator species of forest disturbances can be monitored, providing knowledge on the conservation status of the ecosystem. Remotely sensed data constitute an important source of spatially explicit information on tree species composition. Passive optical sensors such as multispectral and hyperspectral systems have been employed. Hyperspectral sensors, by measuring reflected light from the forest canopy over hundreds of narrow spectral bands, allow the detection of subtle variations in the spectral response of tree species and have been successfully used to accurately map them (Féret and Asner, 2013; Ferreira et al., 2016). However, hyperspectral data have high acquisition and processing costs. Alternatively, the use of satellite images has been investigated (e.g. Cho et al., 2015). Recent technological advances in very high-resolution (VHR) multispectral imagery enable the detection of small objects, such as tree crowns, simultaneously allowing a reliable characterization of the vegetation optical properties. Among the promising VHR multispectral sensors with potential for species identification are WorldView-2 (WV-2) and QuickBird-2 (QB-2). These sensors feature a sub-metric panchromatic band that is useful to detect texture attributes of the tree species and may improve classification accuracy. The aim of this study is to exploit texture descriptors obtained from VHR multispectral images to improve the accuracy of tree species discrimination in a tropical forest area.

2. Materials

2.1 Study area

The study area is the St. Genebra Forest Reserve, which is located in the municipality of Campinas, São Paulo State, southeastern Brazil. The reserve comprises 251.8 ha of a well-preserved submontane semi-deciduous forest formation (Oliveira-Filho & Ratter, 1995) that is subjected to a 5-month dry season (May to September). The forest canopy is highly diverse and composed of deciduous and evergreen species. Floristic surveys that were performed in the area found more than 100 tree species within one hectare (Farah et al., 2014).

2.2 Satellite images

VHR imagery were acquired by QuickBird-2 and WorldView-2 satellite sensors. The images were courtesy of the DigitalGlobe foundation and were radiometrically corrected, sensor corrected and projected using the Universal Transverse Mercator (UTM) projection and the World Geodetic System 1984 (WGS-1984) datum. QB-2, which was launched on October 18th, 2001, is equipped with a panchromatic (PAN) imaging system with 0.6-m spatial resolution and four VNIR bands (450-900 nm) at 2.4-m resolution. WV-2 was launched on October 8, 2009 and features an 8-band system capable of collecting 0.5-m PAN and 2-m multispectral imagery. QB-2 and WV-2 images were collected at the beginning of the dry season in southern Brazil, i.e. May (Table 1).

Table 1. Very high spatial resolution imagery used to classify tropical tree species

| Satellite sensor | Spectral range | Spatial resolution | Acquisition date | Off-nadir view angle |
|-------------------------------|------------------------------|--------------------|------------------|----------------------|
| WorldView-2 | Panchromatic (450-800 nm) | 0.5 m | May 18th 2012 | 2.5° |
| | Coastal (400-450 nm) | 2 m | | |
| | Blue (450-510 nm) | | | |
| | Green (510-580 nm) | | | |
| | Yellow (585-625 nm) | | | |
| | Red (630-690 nm) | | | |
| | Red edge (705-745 nm) | | | |
| | Near-infrared 1 (770-895 nm) | | | |
| Near-infrared 2 (860-1040 nm) | | | | |
| QuickBird-2 | Panchromatic (450-900 nm) | 0.6 m | May 11th 2005 | 1.6° |
| | Blue (450-520 nm) | 2.4 m | | |
| | Green (520-600 nm) | | | |
| | Red (630-690 nm) | | | |
| | Near-infrared (760-900 nm) | | | |

2.3 Field data

In this work, we used the individual tree crown (ITC) dataset of Ferreira et al. (2016), which was produced by visual interpretation and field work data. A total of 255 ITCs were identified, corresponding to seven tree species (Table 2). We manually adjust each ITC according to the QB-2 and WV-2 images and selected only those that were present on both images.

Table 2. Tree species list, number of crowns and pixels on QuickBird-2 (QB-2) and WorldView-2 (WV-2) images.

| Species | Code | Crowns | Pixels QB-2 | Pixels WV-2 |
|--------------------------------|------|--------|-------------|-------------|
| <i>Aspidosperma polyneuron</i> | AP | 23 | 6091 | 8861 |
| <i>Astronium graveolens</i> | AG | 54 | 13,538 | 19,995 |
| <i>Cariniana legalis</i> | CL | 50 | 33,065 | 47,737 |
| <i>Cecropia hololeuca</i> | CH | 39 | 3197 | 5038 |
| <i>Croton piptocalyx</i> | CP | 58 | 10,188 | 15,345 |
| <i>Hymenaea courbaril</i> | HC | 13 | 8699 | 12,545 |
| <i>Pachystroma longifolium</i> | PL | 18 | 1248 | 1797 |
| Total | | 255 | 76,026 | 111,318 |

Source: Adapted from Ferreira et al. (2016)

3. Methods

3.1 Image pre-processing

First, QB-2 and WV-2 images were radiometrically calibrated to radiance using gain and offset values for each band provided by DigitalGlobe. Then, atmospheric correction was applied by using the Fast Line-of-Sight Atmospheric Analysis of Spectral Hypercubes (FLAASH) algorithm (Felde et al., 2003). In this work, we performed image sharpening to explore the very high spatial resolution of the satellite images for tree species classification. We used the nearest neighbor diffusion (NNDiffuse) pan sharpening algorithm (Sun et al., 2014) to sharpen the multispectral data. NNDiffuse salient spatial features while preserve spectral fidelity and proved to perform better both in spatial/spectral quality than tradition methods such as Gram-Schmidt (Sun et al., 2014).

3.2 Texture analysis

Texture attributes may help to increase classification accuracy when the classes present in the image have similar spectral characteristics. Although a universal definition of texture does not exist, it can be understood as regions in an image in which a set of local statistics are either constant, vary slowly or are approximately periodic (Sklansky, 1978). Texture analysis is usually performed by employing quantitative approaches that can be divided into four main categories: structural, statistical, model-based and filter (Bharati et al., 2004). Structural texture analysis is used to describe well-defined patterns of texture such as spaced vertical or parallel lines. Thus, it is limited to describe very regular textures which are uncommon in satellite images acquired over forested areas. Statistical approaches describe texture from the grayscale histogram of an image and extract statistical characteristics from local pixel neighborhood operations. The most used statistical method in remote sensing applications is the gray level co-occurrence matrix (GLCM) (Haralick, 1973). A GLCM is created by calculating how often pairs of pixels with specific values and in a specified spatial relationship occur in an image. Statistical measures such as mean, variance and homogeneity can be computed from a GLCM (Haralick et al., 1973). Model-based techniques create an empirical model of each pixel in the image based on a weighted average of the pixel brightness in its neighborhood. Markov random fields (Cross and Jain, 1983) and fractal models (Keller and Chen, 1989) are examples of such techniques. Filter methods work in the spatial frequency domain by converting the image using the pixel intensity variations. Gabor

and wavelet transforms are examples of filter methods that have been used in image texture analysis. The Gabor transform (Gabor, 1946) allows representing the signal (e.g. the spectral response of a pixel) in the space and frequency domain simultaneously. Texture is usually extracted from a bank of Gabor filters with different spatial frequencies and orientations (Jain and Forrokhnia, 1991). The wavelet transform decomposes the signal into a set of coefficients that represent a measure of intensity of local variations in a given scale or resolution. With the discrete wavelet transform (DWT), the signal is decomposed in a set of dyadic scales by using high-pass and low-pass filters (Mallat, 1989). The output of a DWT decomposition is a set of detail and approximation coefficients. A variety of parameters can be computed from these coefficients, but the most commonly used is the energy feature vector (Zhang et al., 2006).

In this work, we used the pan-sharpened QB-2 and WV-2 to generate statistical and filter texture descriptors. We computed GLCM mean, variance, homogeneity, contrast, dissimilarity, entropy, second moment, and correlation textural features using a 5 x 5 window size. The Gabor filter bank was carried out with six orientations (0°, 30°, 90°, 120° and 150°) and four spatial frequencies (5, 10, 15 and 20 in pixels/cycles), resulting in a total of 20 features. The wavelet analysis was performed using the DWT and the energy feature vector was computed for each pixel. All image processing operations of this section were performed in MATLAB® environment.

3.3 Classification

Labeled pixels from the manually delineated ITCs (section 2.3) were extracted from the QB-2 image to compose a dataset with four reflectance bands, 20 Gabor features, two wavelet energy features and 76,026 samples (Table 2). The same procedure was performed with the WV-2 image, resulting in another dataset with eight reflectance bands, 20 Gabor features, four wavelet energy features and 111,318 pixels (Table 2). These datasets were randomly partitioned into 60% for training and 40% for testing. During this process, the ITC identity was respected, i.e., testing and training pixels of the same species came from different ITCs. Previous studies showed that violations of the ITC identities could overestimate the classification accuracy (Baldeck & Asner, 2014). We trained the Support Vector Machine (SVM; Vapnik, 2000) classifier with the Radial Basis Function (RBF-SVM) kernel and evaluated the model performance on the testing data. The RBF-SVM parameters were chosen using a grid search strategy in the training set (see Ferreira et al., 2016). We repeated the classification procedure 100 times, randomly choosing ITCs to train and test the classifier at each realization. To evaluate if texture descriptors may improve classification accuracy, the experiments were performed using either the reflectance bands alone or combined with GLCM, gabor or wavelet energy features.

4. Results and discussion

Image sharpening performed by the NNDiffuse algorithm yielded good results (Figure 1). For example, the increase from 2-m to 0.5-m in the spatial resolution of the WV-2 image provided a detailed view of the tree crowns and allowed the improved detection of texture patterns. Large tree species such as *Cariniana legalis* and *Aspidosperma polyneuron* tend to have the presence of shadows within the crown caused by their irregular structure. In contrast, species with smaller sizes and with densely foliated crowns, such as *Croton piptocalyx*, show a smoothed appearance (Figure 1). Texture methods may take advantage of such patterns to improve the accuracy of tree species discrimination.

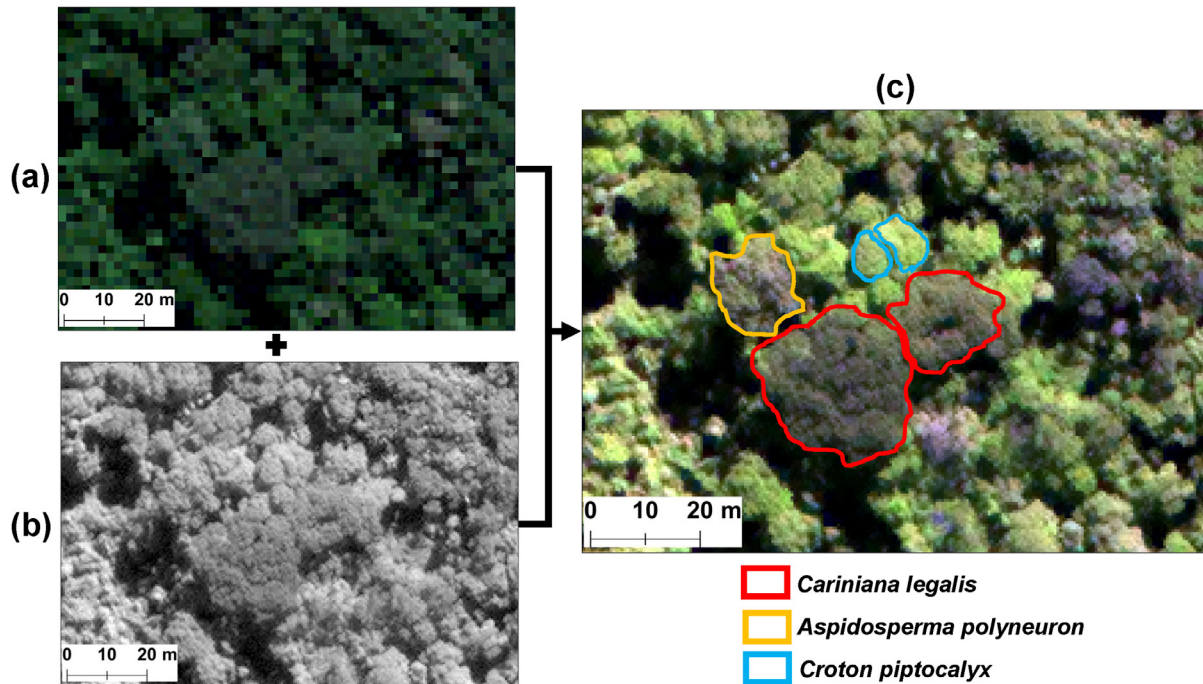


Figure 1. Panchromatic sharpening of the WorldView-2 image. (a) True color composition (R=Red, G=Green, B=Blue) with 2-m spatial resolution. (b) Panchromatic image with 0.5-m spatial resolution. (c) False color composition of the pan-sharpened image (R=Red edge, G=Near-infrared 1, B=Green) with 0.5-m spatial resolution, showing an example of the tree species classified. The images were courtesy of the DigitalGlobe foundation.

WV-2 proved to be more effective than QB-2 to discriminate the species. While the mean of the average accuracy reached 26.6% with the QB-2 reflectance bands, it was raised to 44.8% when the WV-2 bands were used (Figure 2). In general, the inclusion of texture descriptors increased the average accuracy; an exception was the WV-2 reflectance combined with gabor features. The most prominent increase in the average accuracy was observed when GLCM features were incorporated into the classification scheme. More specifically, while the accuracy ranged from 24.6% to 28.2% with QB-2 reflectance and from 40.8% to 48.4% with WV-2 reflectance, the inclusion GLCM features increased the accuracy to the range from 27.6% to 32.2% for QB-2 and from 45.3% to 55% for WV-2.

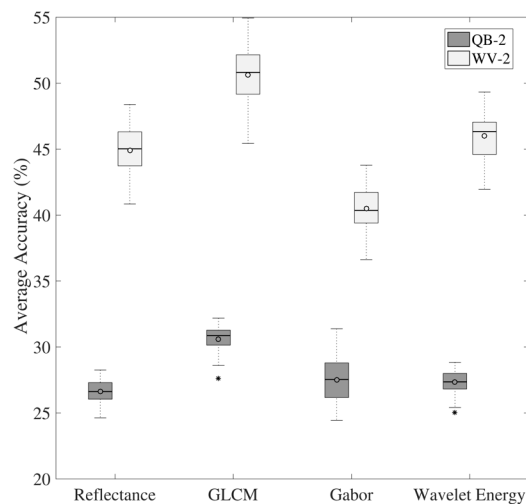


Figure 2. Box-and-whisker plots that show the variability in the average classification accuracy of the studied species. The central lines are the medians. The central dots are the means. The upper and lower quartiles are represented by the edges of the boxes. The dashed line extends to the most extreme data points that are not considered outliers. Outliers are plotted individually. Different texture attributes, such as Gray Level Co-occurrence Matrix (GLCM), Wavelet energy feature and Gabor features, were combined with the original reflectance bands for species classification. The Radial Basis Function Support Vector Machines (RBF-SVM) classifier was used with QuickBird-2 and WorldView-2 imagery. Classifications were repeated 100 times. Training and testing crowns were changed at each realization.

The repetition of the classification process 100 times, changing the crowns used to train and test the classifier at each realization, showed that the accuracy was highly variable for all species (Figure 3). Ferreira et al. (2016) argue that variations on classification accuracy are directly related to both intra- and interspecific spectral variability. GLCM features combined with reflectance bands of WV-2 improved tree species discrimination. The increase in the mean of the classification accuracy exceeded 10% for some species such as *Cecropia hololeuca* and *Hymenaea courbaril* (Figure 3). WV-2 imagery combined with GLCM features were able to detect *Cecropia hololeuca* with 91.8% accuracy, which demonstrate the potential of satellite images to map this species. *Cecropia* is a widespread and abundant pioneer genus of the Neotropics and its presence is an indication of forest disturbance and successional processes (Zalamea et al., 2012). By plotting the variability of the GLCM features for each species, we note that *Cecropia hololeuca* showed peculiar patterns. For example, while the variance feature of the other species did not vary significantly, the variance of *Cecropia hololeuca* was very high (Figure 4).

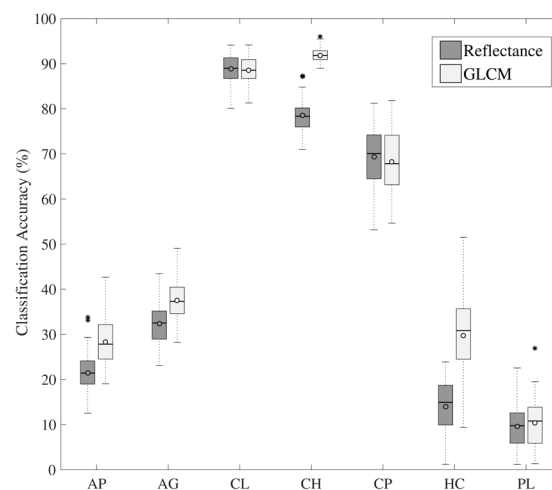


Figure 3. Box-and-whisker plots that show the variability in classification accuracy of the species. The central lines are the medians. The central dots are the means. The upper and lower quartiles are represented by the edges of the boxes. The dashed line extends to the most extreme data points that are not considered outliers. Outliers are plotted individually. Classifications were performed using reflectance bands of the WV-2 satellite alone and combined with Gray Level Co-occurrence Matrix (GLCM) attributes. The Radial Basis Function Support Vector Machines (RBF-SVM) classifier was applied to classify the species. Classifications were repeated 100 times. Training and testing crowns were changed at each realization. AP=*Aspidosperma polyneuron*; AG=*Astronium graveolens*; CL=*Cariniana*

legalis; CH=*Cecropia hololeuca*; CP=*Croton piptocalyx*; HC=*Hymenaea courbaril*; PL=*Pachystroma longifolium*.

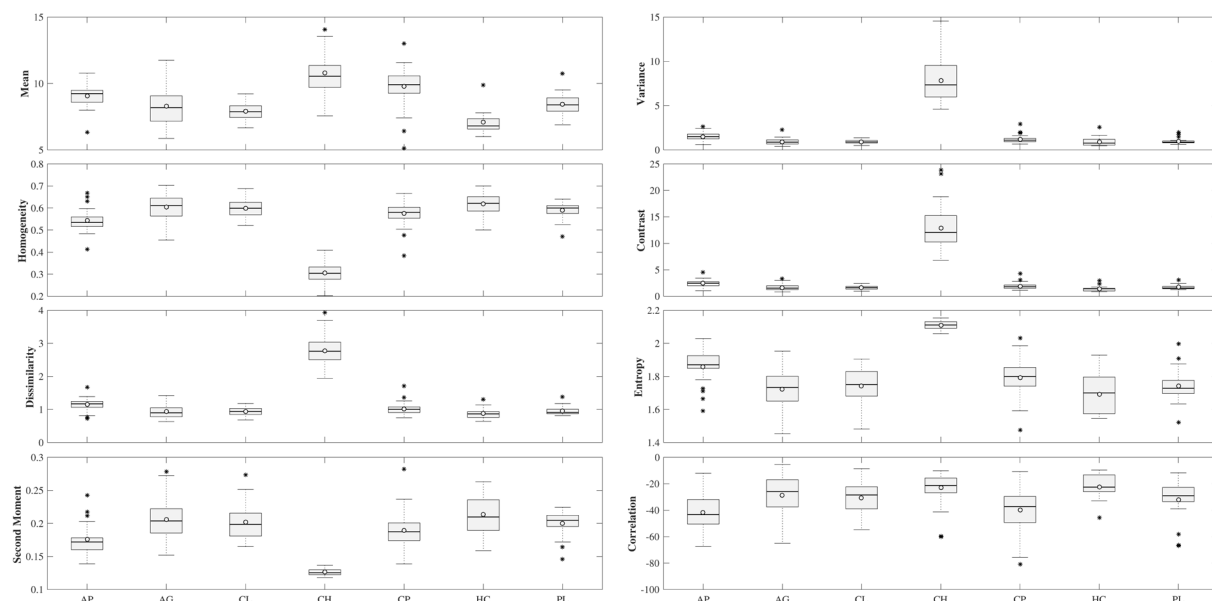


Figure 4. Box-and-whisker plots that show the variability of the Gray Level Co-occurrence Matrix (GLCM) features of the tree species. The central lines are the medians. The central dots are the means. The upper and lower quartiles are represented by the edges of the boxes. The dashed line extends to the most extreme data points that are not considered outliers. Outliers are plotted individually. AP=*Aspidosperma polyneuron*; AG=*Astronium graveolens*; CL=*Cariniana legalis*; CH=*Cecropia hololeuca*; CP=*Croton piptocalyx*; HC=*Hymenaea courbaril*; PL=*Pachystroma longifolium*.

5. Conclusions

In this study we investigated the utility of texture descriptors obtained from VHR images to improve discrimination of tropical tree species. We found that inclusion of GLCM features in the classification process increased accuracy up to 15% for some species. Using WV-2 reflectance bands combined with GLCM attributes, we obtained an average accuracy of 51%. However, some species such as *Cecropia hololeuca* and *Cariniana legalis* were classified with approximately 90% accuracy. We highlight the potential use of WV-2 imagery to monitor tropical forest environments.

Acknowledgments

This work was supported by the São Paulo Research Foundation (FAPESP) grant n° 2013/11.589-5. We gratefully thank the DigitalGlobe foundation for kindly providing the QuickBird-2 and WorldView-2 images.

6. References

- Baldeck, C. A.; Asner, G.P. Improving Remote Species Identification through Efficient Training Data Collection. *Remote Sensing* v. 6, p. 2682-2698, 2014.
- Bharati, M. H.; Liu, J. J.; MacGregor, J. F. Image texture analysis: methods and comparisons. *Chemometrics and intelligent laboratory systems*, v. 72, n. 1, p. 57-71, 2004.

- Cho, M. A., Malahlela, O., Ramoelo, A. Assessing the utility WorldView-2 imagery for tree species mapping in South African subtropical humid forest and the conservation implications: Dukuduku forest patch as case study. **International Journal of Applied Earth Observation and Geoinformation**, v. 38, p. 349-357, 2015.
- Cross, G. R.; Jain, A. K. (1983). Markov random field texture models. **IEEE Transactions on Pattern Analysis and Machine Intelligence**, v. 1, p. 25-39, 1983.
- Farah, F.T.; Rodrigues, R.R.; Santos, F.A.M.; Tamashiro, J.Y.; Shepherd, G.J.; Siqueira, T.; Batista, J.L.F.; Manly, B.J.F. Forest destructuring as revealed by the temporal dynamics of fundamental species—Case study of Santa Genebra Forest in Brazil. **Ecological Indicators**, v. 37, p. 40-44, 2014.
- Felde, G. W.; Anderson, G. P.; Adler-Golden, S. M.; Matthew, N. W.; Berk, A. Analysis of Hyperion data with the FLAASH atmospheric correction algorithm. In: Proceedings of the International Geoscience and Remote Sensing Symposium (IGARSS), Toulouse, 21–25 July 2003, p. 90–92.
- Féret, J.B.; Asner, G.P. Tree species discrimination in tropical forests using airborne imaging spectroscopy. **IEEE Transactions in Geoscience and Remote Sensing**, v. 51, p. 73-84, 2013.
- Ferreira, M. P., Zortea, M., Zanotta, D. C., Shimabukuro, Y. E., & de Souza Filho, C. R. (2016). Mapping tree species in tropical seasonal semi-deciduous forests with hyperspectral and multispectral data. **Remote Sensing of Environment**, v. 179, p. 66-78, 2016.
- Gabor, D. Theory of communication. Part 1: The analysis of information. Electrical Engineers-Part III: Radio and Communication Engineering, **Journal of the Institution of Electrical Engineers**, v. 93, n. 26, p. 429-441, 1946.
- Haralick R. M. Statistical and structural approaches to texture. **Proceedings of IEEE**, v. 67, n. 5, pp. 786-804, 1979.
- Haralick, R.; Shanmugan, K.; Dinstein, I. Textural Features for Image Classification. **IEEE Transactions on Systems, Man, and Cybernetics**, v. 3, n. 6, p. 610-621, 1973.
- Jain, A. K.; Farrokhnia, F. Unsupervised texture segmentation using Gabor filters. **Pattern recognition**, v. 24, n. 12, p. 1167-1186, 1991.
- Keller, J. M.; Chen, S.; Crownover, R. M. Texture description and segmentation through fractal geometry. **Computer Vision, Graphics, and image processing**, v. 45, n. 2, 150-166, 1989.
- Mallat, S. G. A theory for multiresolution signal decomposition: The wavelet representation. **IEEE Transactions on Pattern Analysis and Machine Intelligence**, v. 11, p. 674–693, 1989.
- Oliveira-Filho A.T.; Ratter J.A. A study of the origin of central Brazilian forests by the analysis of plant species distribution patterns. **Edinburgh Journal of Botany**, v. 52, 141–194, 1995.
- Sklansky, J. Image segmentation and feature extraction. **IEEE Transactions on Systems, Man, and Cybernetics**, v. 8, n. 4, p. 907–916, 1978.
- Sun, W.; Chen B.; Messinger, D.W. Nearest Neighbor Diffusion Based Pan Sharpening Algorithm for Spectral Images. **Optical Engineering**, v. 53, n. 1, 2014.
- Vapnik, V.N., 2000. **The Nature of Statistical Learning Theory**, New York: Springer, 2000. 332 p.
- Zalamea, P. C.; Heuret, P.; Sarmiento, C.; Rodríguez, M.; Berthouly, A.; Guitet, S.; Nicolini, E.; Denatte, C.; Barthélémy; Stevenson, P. R. The genus *Cecropia*: a biological clock to estimate the age of recently disturbed areas in the Neotropics. **PloS one**, v. 7, n. 8, e42643, 2012.
- Zhang, J.; Rivard, B.; Sánchez-Azofeifa, A.; Castro-Esau, K. Intra-and inter-class spectral variability of tropical tree species at La Selva, Costa Rica: Implications for species identification using HYDICE imagery. **Remote Sensing of Environment**, v. 105, n. 2, p. 129-141, 2006.